

# Unsupervised Muscle Region Extraction by Fuzzy Decision based Saliency Feature Integration on Thigh MRI for 3D Modeling

Nevrez Imamoglu<sup>1</sup>, Jose Gomez-Tames<sup>1</sup>, Siyu He<sup>1</sup>, Dong-Yun Gu<sup>2</sup>, Kahori Kita<sup>3</sup>, and Wenwei Yu<sup>3</sup>  
<sup>1</sup>Graduate School of Engineering, Chiba University, Japan  
 nevrez.imamoglu@chiba-u.jp, dagothames@chiba-u.jp  
<sup>2</sup>Department of Biomedical Engineering, Shanghai Jiao Tong University, China  
 gudongyun@163.com  
<sup>3</sup>Research Center for Frontier Medical Engineering, Chiba University, Japan  
 yuwill@faculty.chiba-u.jp

## Abstract

*As the first and important step of modeling to explore biomechanical dynamics of the human body, the regions of interest, such as muscles, bones, nerves, and etc., should be extracted from slices of MRI or CT data. Fast and automatic region segmentation would speed up an online process of building physically based models. In this work, a new automatic segmentation model was proposed that utilizes both saliency-on and saliency-off features with simple morphological operations and binary fuzzy decision based fusion. The new model was tested on a dataset of 160 images including two different T1 and one T2 thigh parts. 3D models of the thigh parts were successfully generated with a high segmentation performance, achieving over 90% F-measure values based on 2D comparison and low RMS values of Hausdorff distance based on 3D volumetric comparison. That is adequate for 3D model research since smoothing on manual or automatic segmented images is also applied during 3D construction of the thigh muscle structure. Experimental results showed the possibility of providing automatic muscle segmentation using saliency features for modeling 3D human musculoskeletal system.*

## 1. Introduction

Models of human musculoskeletal system with 3D representation of anatomical details could be used to explore biomechanical dynamics of the human body. For this reason, researchers take advantage of medical images such as MRI and CT to obtain the region of interest to create 3D anatomically based models [1-5]. However, sequential slices are required to build and simulate a 3D model [4, 5]. In addition, datasets from several subjects have to be processed for 3D modeling to be able to make an analysis on different subjects. Therefore, there is an emerging demand on automatic segmentation models for the region of interest to provide time efficiency with acceptable accuracy for the research task [6-11].

Currently, we have been working on the 3D muscle modeling based on the thigh muscle MRI datasets where 2D segmented set of muscle images are required to be able to achieve this goal [4-6]. And, thigh muscles are modeled as one combined structure regardless of individual characteristics of each muscle. Therefore, an estimation that could differentiate muscles, bones and fats is enough to create the model in our application.

Regarding our current research needs, and high amount of data requirement of supervised models [8, 10],

unsupervised methods [6, 7, 9] can be more practical if a faster model with acceptable accuracy is achieved. Thus, in [6], the usability of saliency information was demonstrated on unsupervised thigh muscle segmentation, which is related to visual attention mechanism and can be separated into two feature maps as saliency-on and saliency-off [12, 13, 6]. In the relevant work [6], saliency-on features together with pulse-coupled neural network (PCNN) were employed to enhance a muscle likelihood map by giving promising results compared to existing state-of-art models [6-11] regarding both accuracy and computation time. However, its segmentation performance based on *F-measure* was good only on given T1 dataset. And, the robustness of the segmentation for 3D construction decreased for different MRI settings especially on T2 MRI data. So, parameter adjustment was needed depending on the machine and parameter settings to improve the performance.

To handle the problems in the model [6], in this study, we have proposed a new unsupervised automatic thigh muscle segmentation method which employs both saliency-on and saliency-off features with simple morphological operations and binary fuzzy decision based fusion. Using both saliency on and off features decreased the dependency on intensity by making the method more tolerable to change of data type. Experiments with the proposed model were done for a dataset of 160 images including two different T1 and one T2 thigh segments. 3D models of the thigh parts were successfully generated with the segmentation performance with over 90% *F-measure* values based on 2D comparison and low RMS values of Hausdorff distance based on 3D volumetric comparison, which is useful for 3D model research. Because 3D construction of the thigh muscle structure also includes smoothing on manually or automatically segmented images. Experiments have yielded satisfactory segmentations compared to state-of-the-art models, which is also promising for future work in 3D muscle modeling research by providing fast automatic segmentation of muscles.

## 2. Proposed Model for Muscle Extraction

Proposed model can be separated to several sub-modules; i) region of thigh detection, ii) saliency module that calculates two types of feature map as saliency-on and saliency-off, iii) integration of saliency features by Fuzzy decision module, iv) final enhancement with non-muscle region removal.

## 2.1. Background removal

Initially, foreground and background regions on MRI data should be separated so that only thigh region can be processed to increase the accuracy of the other modules. It is important to remove the background regions since the intensity value maybe similar with the some tissues on the region of interest and any irrelevant information on the background should be avoided. In this work, the foreground region was obtained by the following morphological operations as in Table 1:

Table 1. Pseudo code for background removal

i.	Detect edges using Laplacian of Gaussian (LoG)
ii.	Dilate the edges with a disk of size 3
iii.	Select the longest connected edge (as boundary of the thigh)
iv.	Fill the region of detected boundary
v.	FG = Erode the edges with a disk of size 6
vi.	Image = Image $\cap$ FG

where *Image* is the gray scale thigh MRI data and *FG*, detected foreground region to be used to adjust other features too. The disk size of erode operation was selected bigger than the dilation to remove the possible skin regions that have the similar intensity distribution with the muscle.

## 2.2. Extraction of saliency features on MRI

Saliency computational models aim to generate feature maps that bring out attentive regions, composed of edge to texture level contrasts, by removing the redundant data on the image [12, 13]. Here, our concern is mostly on texture level saliency that would discriminate the regions on the thigh MRI images. Hence, as in [6], we also applied Wavelet transform (WT) based multi-scale saliency model [13] to obtain salient features.

As stated in [12, 6], a gray scale image can give two types of saliency features such as saliency-on and saliency-off information; therefore, local saliency method in [13] was adopted to give these two feature maps separately instead of the combined case. First, WT should be applied to obtain various levels of decomposition that would reveal low-pass approximation data and high-pass details as below [13]:

$$[\mathbf{A}_N, \mathbf{H}_s, \mathbf{V}_s, \mathbf{D}_s] = WT_N(\mathbf{I}) \quad (1)$$

where  $\mathbf{I}$  is MRI in Fig.1(a) and normalized to {0-1},  $WT(\cdot)$  is the wavelet decomposition for scaling level  $s$  and  $s \in \{1, \dots, N\}$ ,  $N$  is coarsest level of decomposition,  $\mathbf{A}$  is the approximation signal of  $N^{\text{th}}$  level decomposition, and the horizontal, vertical and diagonal details,  $\mathbf{H}_s$ ,  $\mathbf{V}_s$ ,  $\mathbf{D}_s$ , are gained respectively.

The saliency-on and saliency-off features were generated from inverse-WT (IWT) of details for defined levels [6, 13] as in (2) and (3) respectively [6, 13]:

$$S_{ON}(x, y) = \sum_{s \in \{N-2:N\}} F_{ON}\left(IWT_s\left([\cdot], \mathbf{H}_s^c, \mathbf{V}_s^c, \mathbf{D}_s^c\right)\right) \quad (2)$$

$$S_{OFF}(x, y) = \sum_{s \in \{N-2:N\}} F_{OFF}\left(IWT_s\left([\cdot], \mathbf{H}_s^c, \mathbf{V}_s^c, \mathbf{D}_s^c\right)\right) \quad (3)$$

where  $S_{ON}$  (Fig.1 (b)) is the saliency-on map that repre-

sents generally non-muscle regions,  $F_{ON}(\cdot)$  is the process considers the positive values of IWT operation to get  $S_{ON}$ ,  $S_{OFF}$  (Fig.1 (c)) is the saliency-off map that represents mostly regions on the muscle area,  $F_{OFF}(\cdot)$  is the process considers the negative values of IWT operation to get  $S_{OFF}$ , and both  $S_{ON}$  and  $S_{OFF}$  were adjusted with  $FG$  by neglecting values out of the foreground region and scaled to {0-1} range.

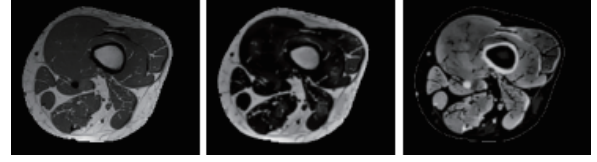


Figure 1. (a) MRI thigh image sample (b) saliency-on feature map (c) saliency-off feature map

Even though, both feature maps seems to detect non-muscle and muscle regions respectively, obviously, both saliency feature maps consist of true and false detections so combining these feature maps and applying morphological operations can be a fast solution to extract the muscle region roughly to satisfy input data for 3D construction.

## 2.3. Extraction of saliency features on MRI

The next step is to combine saliency on and off features to create a muscle region estimation. To be able to distinguish background from the darker area of the saliency-on map, the complement image of saliency-on feature was taken after normalization between {0-1}.

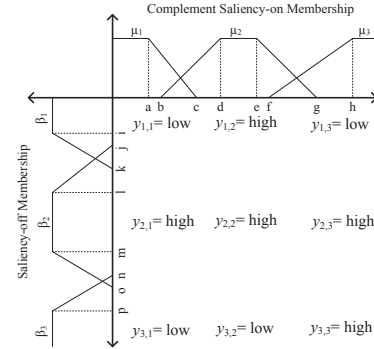


Figure 2. Fuzzy membership parameters and weights for integration

Instead of linear combination, a rule based approach is applied that can provide non-linearity on decision process during fusion of two feature maps. This is achieved by a simple binary Fuzzy decision operation where the membership function parameters and their respective fuzzy weights can be seen in Fig.2 [14, 15].

In Fig.2,  $a$  to  $h$  are the membership parameters of the complement saliency-on membership functions  $\mu_i$ ,  $i$  to  $p$  are the membership parameters of the saliency-off membership functions  $\beta_j$ , and  $y$  is the fuzzy weights corresponding to the decision based on two membership functions' relation. With the membership values, the output of the fuzzy decision module was given in Eq.(4) [14, 15]. And the membership functions of complement saliency are given through (5) to (7) [14]. The saliency-off membership values  $\beta$  can also be calculated with similar modalities since they are using similar functions with difference of parameter values as in Fig.2. The output  $R$  in

(4) is given in Fig.3(b) where it can be seen that the fuzzy output still includes some part of bone structure and some misdetections which can be handled by simple morphological operations as describe in next section. Using fuzzy based on saliency features, we simply created a rough estimation of the muscle region which requires enhancement to obtain muscle regions by removing the irrelevant parts such as bone or fat tissues.

$$R = \frac{\sum_x \sum_y \min(\mu_x, \beta_y) y_{x,y}}{\sum_x \sum_y \min(\mu_x, \beta_y)}; x, y \in \{1, 2, 3\} \quad (4)$$

$$\mu_1 = \max\left(0, \min\left(1, \frac{c - S_{on}}{c - a}\right)\right) \quad (5)$$

$$\mu_2 = \max\left(0, \min\left(\min\left(\frac{S_{on} - b}{d - b}, 1\right), \frac{g - S_{on}}{g - e}\right)\right) \quad (6)$$

$$\mu_3 = \max\left(0, \min\left(1, \frac{S_{on} - f}{h - f}\right)\right) \quad (7)$$

## 2.4. Extraction of the muscle region

Fuzzy saliency feature integration gives a rough estimation of the muscle region that should be enhanced by removing the bone and fat components from the extracted rough muscle template. Using the procedure in Table 2, fuzzy output in Fig.3 (b) can be further enhanced to yield the final segmentation result given in Fig.3 (c) for the sample thigh MRI data in Fig.3(a). Then, 3D construction of the segmented images is done as in Fig.3(d), which can be used for model analysis after adjusting to decrease complexity as given in Fig.3(e) for simulation study.

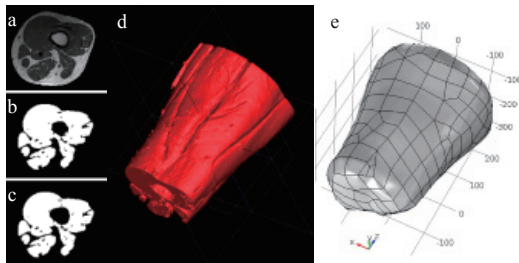


Figure 3. (a) MRI thigh image sample (b) fuzzy binary output of saliency integration (c) final segmentation result (d) 3D construction of sequential data (e) Smoothed 3D data for model analysis

Table 2. Pseudo code for muscle region extraction

i.	Extract possible bone regions based on intensity value and saliency-off feature with respective thresholds
ii.	Find the structure with the biggest hole inside that is the bone part
iii.	Select the bone component and fill the hole
iv.	Find the possible fat regions from saliency-on with threshold
v.	Remove skeleton and fat region found from fuzzy binary output of (4) which will yield the final segmentation result

## 3. Experimental results and discussion

In this work, 30 T1, 30 T2 from [5] and 100 T1 MRI data from [6] were used to make experiments, in which all three data groups are sequential thigh parts. So, 3D

muscle structure could be constructed by the segmentation results. *Matlab*<sup>®</sup> was used for segmentation with a processing time of approximately 10 seconds per image for 768x504 pixels, and the 3D model was reconstructed in *ITK-Snap*. For performance evaluation, manual segmentation of each image was performed by the expert in the field, which constitutes ground truth (GT) images of the dataset. Firstly, GTs are compared with the segmentation results of the proposed model quantitatively by applying *F-measure* metric that is the harmonic mean of *precision* and *recall* values [13, 6].

Several state-of-the-art models [6-11] with evaluation metrics and performances are given in Table 3. Unfortunately, the algorithms or data were not available to test their model using data from [5, 6]; therefore, the results were taken from each references. However, the performance of the proposed algorithm using salient features is still comparable to these studies. In Table 3, each reference can be defined as [6]: i) [7] is fuzzy C-means segmentation (FCMS), ii) [8] is surface expansion based segmentation (SES), iii) RMLS [9] is unsupervised recursive and multilevel algorithm that considers shaped histograms, adaptive threshold and connectivity, iv) [10] is the shape prior knowledge based segmentation (SPKS), v) [11] is multi-scale human-MIRALab based on automatic and quasi-automatic multi-resolution simplex meshes (MRSM), iv) saliency-on muscle segmentation (SOMS) is relevant model [6]. Supervised or quasi-automatic models SES [8], SPKS [10], and MRSM [11] may have better results compared to the remaining unsupervised approaches including the proposed model. However, it is very difficult to obtain huge amount of training data with defined tissue regions, and human interaction can increase the segmentation time, especially on continuous slices to construct 3D model. On the other hand, our unsupervised model has promising result by having more than 0.92 F-measure from all three data, which is better than FCMS [7] and similar to SOMS [6].

Table 3. Quantitative Performance Other Models

Compared Models	Evaluation	Quantitative Results	Computation Time
FCMS [7]	Accuracy <sup>1</sup>	≈0.91	NA
SES [8]	Accuracy <sup>1</sup>	≈0.94	NA
RMLS [9]	CP-Rate <sup>2</sup>	over %90	≈ 300 s/img
SPKS [10]	DSC <sup>3</sup>	≈0.95	NA
MRSM [11]	Distance	1.5 mm	≈ 12 s/img
SOMS*[6]	F-measure	≈0.92	≈ 1 s/img
Linear model*	F-measure	≈0.91	≈ 1 s/img
Fuzzy Model*	F-measure	≈0.92	≈ 10 s/img

\*Tested using the dataset in this study, <sup>1</sup>Accuracy: Recall, <sup>2</sup>Coincidental pixels rate, <sup>3</sup>DSC: Dice similarity coefficient



Figure 4. (a) T2 sample image (b) segmentation result of [6] (c) segmentation result of proposed model

For the 30 T1, 30 T2 data [5], and 100 T1 data [6], *F-measure* values were observed as 0.9164, 0.9166, and 0.9402 respectively where 100 T1 data had the best score due to its higher image quality. Comparing the relevant

work [6] with the proposed model, even though the model [6] is faster and overall results of [6] and proposed algorithm were very similar as being 0.92 average *F-measure* of all data, proposed model was better for the T2 images without any failure; on the other hand, work in [6] was not robust to T2 dataset in which it failed in some of the data that is hard to use in 3D modeling by requiring more manual processing time on the segmentation results (Fig.4). Also, we tried linear combination of two features instead of fuzzy. Linear approach yielded *F-measure* performances as 0.8861 on 30 T1, 0.9296 on 30 T2, and 0.9229 on 100 T1 data. Despite being an average of 0.91, its *F-measure* performance deviations are too much and the segmented regions are not very consistent, especially on 30 T1 data with 0.88 *F-measure* performance. On the other hand, fuzzy combination results are more consistent in all three datasets.

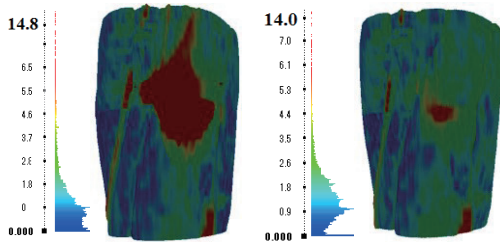


Figure 5. Hausdorff distance for (a) T1 data set and (b) T2 data set. The error is larger in the rectus femoris in T1 and was diminished in T2.

Also, 3D models constructed from manual and automatic segmentations were compared using Hausdorff distance (two sided) between the vertices of the meshed models [16]. The better 3D model was for 100 T1 data, which has the lowest mean (1.69) and lowest RMS (3.11) Hausdorff distance values between the three data sets. In the case of the 30 T2 and 30 T1 data sets of [5], the mean values were 2.05 and 2.00, and RMS of 3.44 and 3.54, respectively. Fig.5 illustrates the locations where the error is higher (red) and lower (blue). These results showed that the proposed model can tolerate the differences for different MRI data. Especially, the *F-measure* results are better when the image resolution and quality is higher concerning the performance difference between 30 T1 and 30 T2 data [5], and 100 T1 data [6] where 100 T1 data of [6] has better quality compared to the data in [5]. In conclusion, unsupervised thigh muscle segmentation was achieved with a promising accuracy and acceptable computation time.

#### 4. Conclusion

In this study, saliency-on and saliency-off feature integration was proposed based on a fuzzy decision rule to demonstrate the reliability of saliency information on unsupervised segmentation model. All the datasets have performance values over %90 that is satisfactory and beneficial to 3D anatomically based modelling. However, as a future work, there is still place for improvement such as decreasing resolution effect, increasing accuracy and data, or better bone and fat region detection algorithms.

#### References

- [1] J. Fernandez, M. Buist, D. Nickerson, P. Hunter, "Modeling the passive and nerve activated response of the rectus femoris muscle to a flexion loading: a finite element framework," *Medical Engineering&Physics*, vol. 27, pp. 862-870, 2005.
- [2] R. Kinugasa, D. Shin, J. Yamauchi, C. Mishra, J. Hodgson, "Phase-contrast MRI reveals mechanical behavior of superficial and deep aponeuroses in human medial gastrocnemius during isometric contraction," *Journal of Applied Physiology*, vol. 105, pp. 1312-1320, 2008.
- [3] M. Böl, H. Stark, N. Schilling, "On a phenomenological model for fatigue effects in skeletal muscles," *Journal of Theoretical Biology*, vol. 281, pp. 122-132, 2011.
- [4] J. Gomez-Tames, J. Gonzalez, W. Yu, "A simulation study: Effect of the inter-electrode distance, electrode size and shape in Transcutaneous Electrical Stimulation," *Proc. 34<sup>th</sup> Annu. Int. Conf. of the IEEE Engineering in Medicine and Biology Society (EMBC)*, pp.3576-3579, 2012.
- [5] F-J Pettersen, J. O. Hogetveit, "From 3D tissue data to impedance using Simpleware ScanFE+IP and COMSOL Multiphysics – a tutorial," *Journal of Electrical Bioimpedance*, vol. 12, pp. 13-22, 2011.
- [6] N. Imamoglu, J. Gomez-Tames, J. Gonzalez, D. Gu, and W. Yu, "PCNN Segmentation and Bottom-Up Saliency-On Feature Extraction for Thigh MRI based 3D Model Construction," *Journal of Medical Imaging and Health Informatics*, vol.4, pp.1-10, 2014.
- [7] H. Kang, A. Pinti, L. Vermeiren, A. Taleb-Ahmed, X. Zeng, "An automatic FCM-based method for Tissue classification: Application to MRI of Thigh. 1<sup>st</sup> Int. Conf. on Bioinformatics and Biomedical, (2007), pp.510-514, Wuhan, China.
- [8] A. Pinti, P. Hedoux, H. Kang, A. T. Hamed, "An automated pixel classification method using surface expansion: Application to MRI image sequence. *IMACS Multiconference on Computational Engineering in Systems Applications*, (2006), pp.1514-1519, Beijing, China.
- [9] L. Urricelqui, A. Malanda, A. Villanueva, "Automatic segmentation of thigh magnetic resonance images," *WASET Congress (58)*, 2009, pp.979-985.
- [10] S. Andrews, G. Hamarneh, A. Yazdanpanah, B. HajGhanbari, W.D. Reid, "Probabilistic multi-shape segmentation of knee extensor and flexor muscles," *Lecture Notes in Computer Science*, vol.6893, pp. 651-658, 2011.
- [11] B. Gilles, N. Magnenat-Thalman, "Musculoskeletal MRI segmentation using multi-resolution simplex meshes with medial representations," *Medical Image Analysis*, vol.14, pp.291-302, 2010.
- [12] S. Frintrop, "VOCUS: A visual attention system for object detection and goal directed search," *Lecture Notes in Artificial Intelligence (LNAI)*, Springer, 2006.
- [13] N. Imamoglu, W. Lin, Y. Fang, "A saliency detection model using low-level features based on Wavelet transform," *IEEE Trans. on MultiMedia*, vol.15, no.1, pp.96-105, 2013.
- [14] K.M. Passino, S. Yurkovich, *Fuzzy Control*, Addison-Wesley Longman Inc., Menlo Park, California, pp. 23-99,1998.
- [15] N. M. Thanh and M.-S. Chen, "Image denoising using adaptive neuro-fuzzy system. *Int. Journal of Applied Mathematics*, vol. 36, no. 1, pp. 1-11, 2007.
- [16] Cignoni, Paolo, Claudio Rocchini, and Roberto Scopigno. "Metro: measuring error on simplified surfaces," *Computer Graphics Forum*, vol.17, no.2, Blackwell Publishers, 2001.